Steady viscous flow inside deep, shallow and skewed cavities by an implicit Navier-Stokes solver

Hassan Fayyaz, Abdullah Shah *

Department of Mathematics, COMSATS Institute of Information Technology, Park Road Chak Shahzad, Islamabad, Pakistan

ABSTRACT

In this paper, accurate and efficient calculations of the flow inside different types of cavities are presented. The incompressible Navier-Stokes equations are expressed in generalized curvilinear coordinates using artificial compressibility method. The governing equation in conservative form is solved numerically using an upwind compact finite difference scheme. The solution algorithm for solving the resulting linear system of equation is approximate factorization based ADI scheme. The computed results are compared with the results in the literature and the agreement is good. Also the presence of multiple solution and critical value of aspect ratio and Reynolds number for two sided cavity calculated and compared.

1. Introduction

The problem of steady incompressible viscous flow within different cavities is of primary importance in fluid dynamics. The development of improved methods for solving the classical lid driven cavity problem has been an attractive research problem in computational fluid dynamics for many years. Being simple in geometry, the lid driven cavity contains a variety of interesting phenomena in it. Classical lid driven cavity problem was then extended to deep one sided cavity problem by Cortes and Miller (1994) who studied the effect of Reynolds number up to 10,000. Patil et al. (2006) have investigated the effect of Reynolds number for deep cavity with one sided wall motion, having aspect ratio 2 and 4. They also gave the effect of aspect ratio on secondary vortex formation. Latter, Omari (2013) have studied the effect of Reynolds number as well as aspect ratio. Perumal and Dass (2013) and Perumal (2012) have predicted that lid driven cavity with different aspect ratios can exhibit all phenomena of incompressible flows. The presence of primary and secondary eddies, flow with different aspect ratios, exploiting different boundary conditions have made the lid driven cavity flows as an attractive choice for the comparison of the numerical schemes. Kuhlmann et al. (1997) have studied the flow inside two sided cavity. They

investigated the asymmetric solution inside two sided channel with facing walls. Arun and Satheesh (2015) studied the flow inside deep parallel and antiparallel cavity with aspect ratio 1, 2 and 4. The two sided cavity flow phenomena in square and rectangular cavities have further studied by Perumal and Dass (2010). They investigated the flow inside deep, two sided lid driven cavity with aspect ratio 2 and 5 while Prasad and Dass (2016) studied the flow inside two sided deep cavity and phenomena of flow bifurcation was introduced for various kinds of two sided square cavities. Along with the benchmark results, two sided cavity have many industrial applications as well. Perumal et al. (2014) described many industrial applications of two sided in lid driven cavity in the field of manufacturing of processes. Non-linear phenomena of flow inside cavity exhibit multiple steady solutions at high Reynolds number. Wahba (2009) have proposed the multiple solutions for a single Reynolds number with non-facing cavity. Luo and Yang (2007) studied multiple solution phenomena for two sided facing cavity with parallel wall motion, anti-parallel wall motion and non-facing wall motion. They calculated the critical and threshold values for a single Reynolds number and aspect ratio for which asymmetric solution is obtained.

The objectives of the present work are the following: i) implementation of an implicit high-order upwind compact scheme in curvilinear coordinates for simulations of rectangular 2D cavities, specifically for deep-cavities whose aspect ratio > 1, shallow cavity with aspect ratio < 1, cavity with two sided wall motion and deep cavity skewed at various angles; ii) to interpret the results

with particular focus on the structure of the primary- and corner-eddies; iii) to investigate the critical value of aspect ratio and Reynolds number; and iv) to study the critical value for non-facing two sided cavity.

The rest of the paper is organized as follows. Section 2 describes the numerical procedure, Section 3 discusses the numerical examples and Section 4 concludes this paper.

2. Governing equations and numerical discretization

The governing equations are the two-dimensional incompressible Navier-Stokes equations, which are written in conservative form in generalized curvilinear coordinates ξ and η using artificial compressibility method;

$$\frac{\partial \hat{Q}}{\partial \tau} + \frac{\partial \hat{E}}{\partial \xi} + \frac{\partial \hat{F}}{\partial \eta} - \frac{1}{Re}\left(\frac{\partial \widehat{E_v}}{\partial \xi} + \frac{\partial \widehat{F_v}}{\partial \eta}\right) = 0, \qquad (1)$$

where τ is pseudo-time or iteration parameter due to the artificial compressibility formulation Chorin (1997), $\hat{Q}$ is the solution vector in the transformed plane, while the vectors $\hat{E}$, $\hat{F}$ are viscous fluxes and $\widehat{E_v}$ and $\widehat{F_v}$ are inviscid fluxes respectively i.e.,

$$\hat{Q} = \frac{1}{J}(p, u, v)^t,$$
$$\hat{E} = \frac{1}{J}(\beta U, uU - \xi_x P, vU + \xi_y P)^t,$$
$$\hat{F} = \frac{1}{J}(\beta v, uv + \eta_x P, vV + \eta_y P)^t, \text{ and}$$

$$\widehat{E_v} = \frac{1}{J}(\xi_x E_v + \xi_y F_v)^t, \ \widehat{F_v} = \frac{1}{J}(\eta_x E_v + \eta_y F_v)^t,$$

β is the artificial compressibility parameter that controls convergence of the method, Re is the Reynolds number and J is the Jacobean of transformation, U and V are the contra-variant velocity components and ξ_x and η_x are the metrics.

In artificial compressibility method, adding a pseudo-time derivative of pressure to the continuity equation circumvents the difficulty of the pressure decoupling in the incompressible Navier-Stokes equations. The resulting system of equations is iterated in pseudo-time until the mass conservation constraint is satisfied. The method leads to hyperbolic and hyperbolic-parabolic equations for inviscid and viscous incompressible flows, respectively. Therefore, numerical schemes developments for compressible flows can be easily transferred to incompressible flows. The aim of the present work is to use an implicit backward finite difference scheme for discretization of pseudo-time derivative, third-order upwind compact scheme for convective terms and fourth-order central compact scheme for the viscous terms. The metric terms are discretized with six-order central finite difference scheme. The discretized equations are solved using Beam-Warming approximate factorization based alternate direction implicit (ADI) scheme as detailed in (Shah et al., 2009; 2012).

3. Results and discussions

In this section, we investigate the viscous flow in some cavities like non-facing cavity, flow in a deep and shallow cavity, flow inside a two-sided cavity and flow in a two-sided skewed cavity. The physical domain in xy^- plane is transformed into the computational domain (ξ, η) by the following coordinate transformation (Nayak et al., 2015).

$$\xi = x - y \cot \alpha \qquad (2)$$
$$\eta = y/\sin \alpha \qquad (3)$$

3.1. Flow in a deep-cavity

To study the flow phenomena inside the deep-cavity with different aspect ratio, we keep the skewed angle $\alpha = 90°$ in formulae (2) and (3). The top lid moving with constant speed, while all other walls are stationary. The grid size is 101 per unit length while the aspect ratio is 1.5, 2, 3 and 4. In Fig. 1, the comparison of computed results for normalized "u" versus "y" with the results of Cortes and Miller (1994) and Omari (2013) are presented for cavities having aspect ratio of 3 and 1.5 respectively.
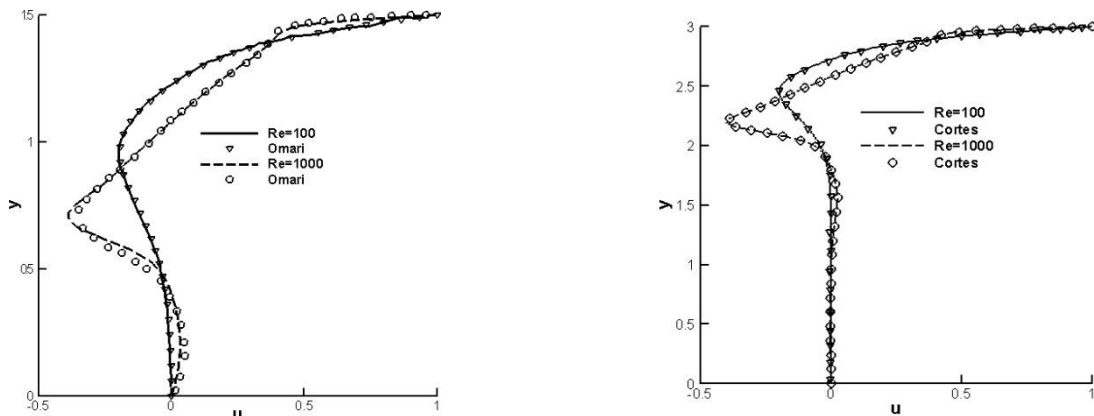

Fig. 1: Comparison of normalized u versus y for Re= 100 and Re= 1000, (left) aspect ratio= 1.5 (right) aspect ratio= 3.0

To further verify our method, the deep-cavities with aspect ratios of 1.5, 2, 3 and 4, are also studied with different Reynolds numbers. It is observed that the number of counter rotating vortices are

produced under the moving lid depends directly on Reynolds number. As Reynolds number increases, the center of primary eddy moves in downward direction and at higher Reynolds number, the number of counter rotating vortices increases that depend upon both Reynolds number and aspect ratio. For the cavity with aspect ratio 2 or higher, the difference between two consecutive eddies is found to be 0.73 for Re= 50 and has good agreement with the result of Patil et al. (2006).

For cavity having aspect ratio 2, top primary vortex location is 1.58267 and location for secondary vortex is 0.84864 so the difference in location for two consecutive vortices is 0.73403 for Re= 1000 which qualitatively agrees with the result of Patil et al. (2006). Also for aspect ratio=4.0 top primary vortex is located at location 3.61337 and secondary vortex lies at the location 2.86029, so the difference between consecutive locations is 0.75261. For the aspect ratio of 1.5, the flow topology consists of only one eddy with two small corners eddies at low Reynolds number. When the aspect ratio increases to a certain aspect ratio, two corner eddies enlarge and merge to form a secondary vortex for the same Reynolds number i.e., Re= 50. The critical value for merging of two secondary eddies is 1.71 and is verified for the present scheme which is shown in Fig. 2 which agrees with the result of Patil et al. (2006).
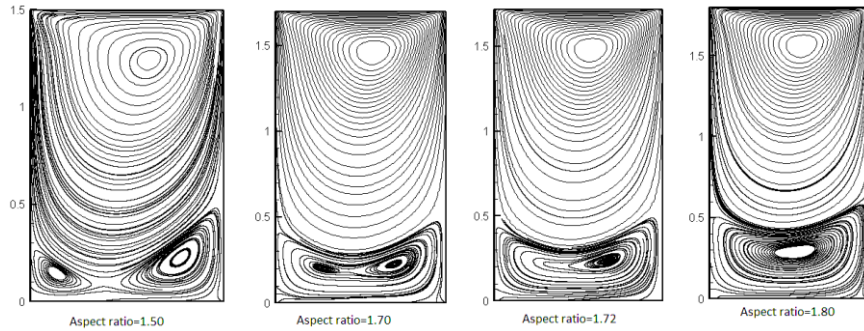

Fig. 2: Formation of secondary vortex for Re=50 for different aspect ratio i.e., Aspect ratio= 1.5, Aspect ratio=1.70, value below critical value, Aspect ratio=1.72, value above critical value formation of one vortex, and Aspect ratio= 1.80

3.2. Flow in a shallow-cavity

In this case, the aspect ratio is kept less than one i.e., length of the cavity is greater than its depth. In the first part, the top wall of the cavity is moved with unit speed along x-direction. Fig. 3 in left shows the comparison plots of v versus x, with the results of Omari (2013) while in the Fig. 3 in right shows, the comparison of u versus y for cavity having aspect ratio 0.50 and Re= 100 and Re=1000 with Perumal and Dass (2013).
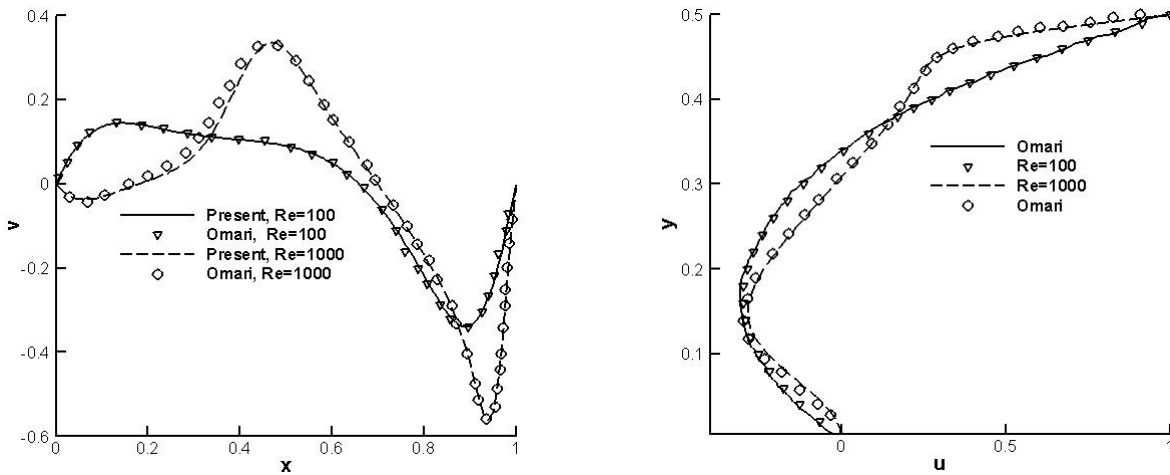

Fig. 3: For aspect ratio 0.5 (left) Comparison of v versus x for different Re with Omari (2013), (right) Comparison of u versus y for different Re with Perumal and Dass (2013)

The Fig. 4 shows the streamlines for the shallow cavity with aspect ratio= 0.5, that shows the qualitative comparison of present scheme is good as compared with the reference Perumal and Dass (2013).
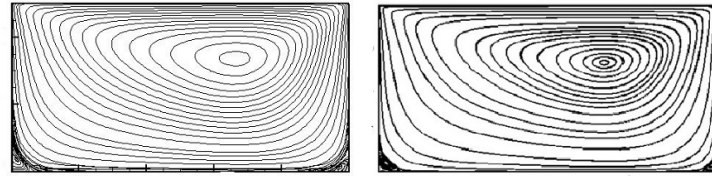
Fig. 4: Streamlines for cavity having Aspect ratio 0.5, for Left=present, right= Perumal and Dass (2013)

In the second case of this subsection, the top and bottom walls of the cavity are moved. For the shallow parallel lid driven two sided cavity, aspect ratio plays an important role. We have observed that with Re= 600, for the aspect ratio between 0.56 and 0.91, two solution one symmetric and another asymmetric are obtained. However, for aspect ratio greater than 0.91, the asymmetric solution ceases off which agrees with the results of Prasad and Dass (2016) and are shown in Fig. 5.
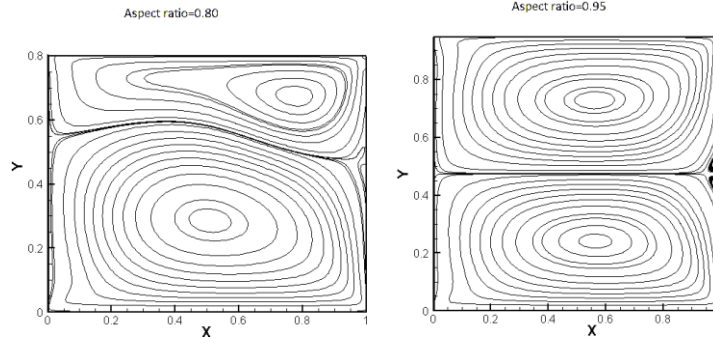

Fig. 5: Aspect ratio effect for the shallow two sided parallel cavity for Asymmetric solution for aspect ratio =0.80 and Symmetric solution for aspect ratio=0.95

3.3. Flow in a two sided deep-cavity

When we generate a cavity using Eqs. 2 and 3 with the skewed angle $\alpha = 90°$ and moving both top and bottom walls, the cavity is termed as two sided cavity. An extensive work to investigate flow patterns in two sided cavity was done by Perumal and Dass (2013, 2010). In Table 1, the "y" location of vortices is presented for two sided deep cavity parallel and antiparallel cavity. For the parallel cavity vortex location is compared with the Arun and Satheesh (2015) for Re=100 and for antiparallel cavity the vortex location in y direction is presented for Re=2000. It is observed in Table 1 that for antiparallel two sided cavity with aspect ratio=2.0, there are three vortices and for cavity having aspect ratio 4.0, there are five vortices.

Table 1: Vertical "y" location of vortices for two sided deep parallel and antiparallel cavity having aspect ratio 2 and 4 compared with Perumal et al. (2014)

(a) Parallel cavity	Re=100				
Aspect ratio (Ref)	**I**	**II**	**III**	**IV**	**V**
2.0 (Agarwal)	0.27	1.73	-	-	-
(Present)	0.28	1.74	-	-	-
4.0 (Agarwal)	0.26	1.60	2.38	3.74	-
Present	0.26	1.57	2.37	3.72	-
(b) Anti parallel cavity	Re=2000				
2.0 (Agarwal)	0.26	1.00	1.74	-	-
Present	0.25	1.00	1.73	-	-
4.0 (Agarwal)	0.45	1.25	1.99	2.75	3.56
Present	0.45	1.25	2.00	2.76	3.57

3.4. Flow in a non-facing square cavity

In this subsection, we focus on the cavity with skewed angle of 90° with non-facing (upper and left walls). In the left hand side of Fig. 6, the streamlines for the square cavity with non-facing wall motion are shown for Re=100. The locations of vortices are also presented. It is observed that increasing the Reynolds number increases the vortex size. In the right hand side of Fig. 6, the plot of u versus y is given for comparison with the results of Perumal and Dass (2010).

Increasing the Reynolds number increases the size of vortices as long as the value of the Reynolds is below critical value. It is verified that the critical value of Reynolds number for non-facing square cavity is 1073, after which the phenomena of bifurcation arises. The geometric center of the non-facing driven cavity is no longer zero and it produces multiple solutions at for a fixed Reynolds number. For each Reynolds number one symmetric and one asymmetric solution are produced. The asymmetric solution above the critical value of the Reynolds numbers is stable while the symmetric solution is unstable which is shown in Fig. 7. The results are compared with the results of Wahba (2009) in the above part of Fig. 7, while the results with same Reynolds number are presented with the below part

of Fig. 7. It is observed that the current scheme gives improved results than that of Wahba (2009) results.
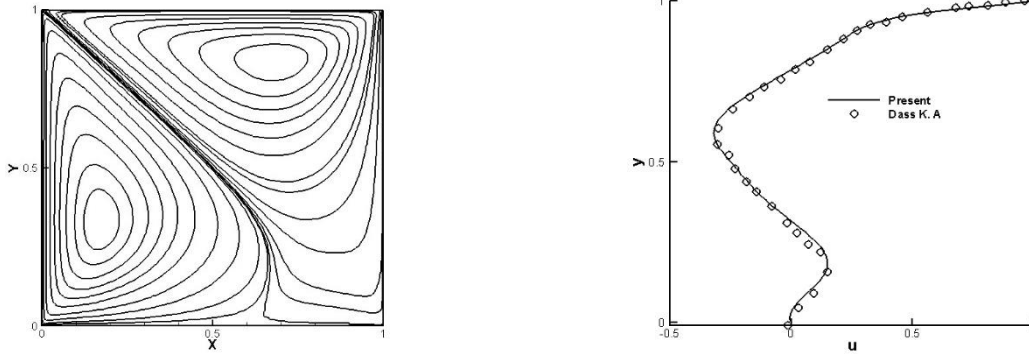

Fig. 6: (left) The geometry with streamlines for non-facing cavity at Re=100 (right) Plot of u versus y for non-facing cavity at Re=500, compared with (Perumal and Dass, 2010)
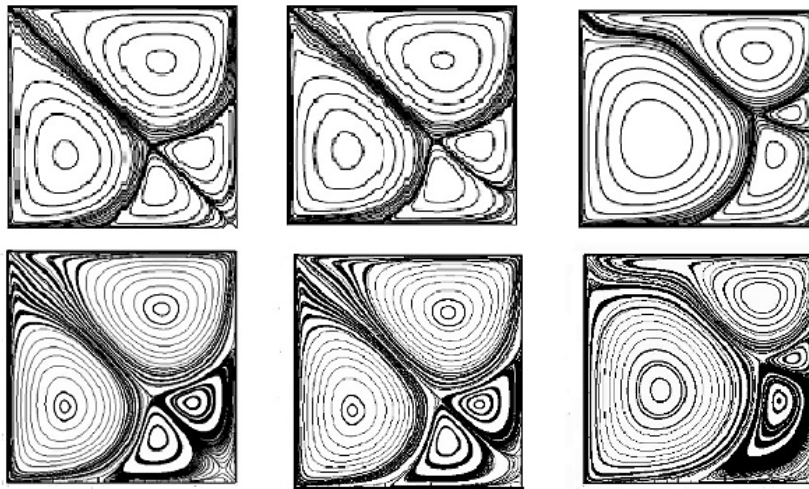

Fig. 7: Presence of asymmetric solution above the critical value for non-facing cavity compared with Wahba (2009) above, and present results are given below for Re= 1000, Re=1075 and Re=1500 left to right, respectively

3.5. Flow in a two sided skewed-cavity

In this section, results for the variation of skew angle α in Eqs. 2 and 3 are presented. The aspect ratio for the cavity is also kept greater than one. The cavity is termed as deep skewed-cavity. In the first part of this subsection, the flow plots of normalized "u" versus "y" are shown in Fig. 8 for different aspect ratio. In first part of Fig. 8, the effect of depth for the deep two sided anti parallel skewed cavity is presented and in the second part of the Fig. 8, the plots of "u" versus "y" for parallel skewed driven deep cavity is presented. The Fig. 8 shows that flow behave similar manner with only difference in depth. Here the skew angle is fixed at 45°.

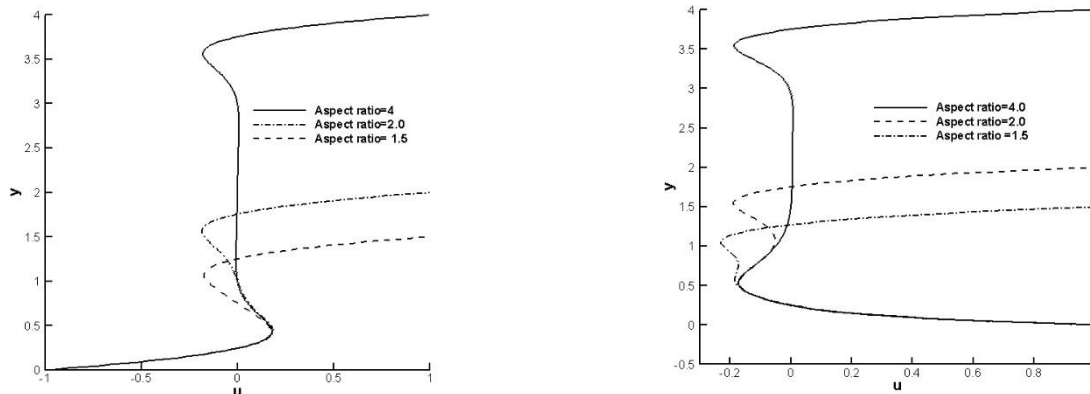**Fig. 8:** For skew angle 45°, plots of u versus y for different aspect ratio (left) For antiparallel deep two sided cavity(right) Parallel deep two sided cavity

The streamlines pattern for skew angle 45° and 60° are presented for both shallow and deep skewed-cavities with aspect ratio 0.75 and 1.5. The top and bottom walls are moving in parallel

direction to each other. The computed results are presented in Fig. 9 which shows that asymmetric solution is obtained for the cavity with aspect ratio = 0.70 at Re= 1000. The presence of asymmetric solution for shallow-cavity is dependent on aspect ratio as well as on Reynolds number. For the two sided cavity, the critical value for aspect ratio and Reynolds number is same as given in section 3.2.

In the Fig. 10, the streamlines pattern for antiparallel-cavity with aspect ratio 1.5 and 2.0 are shown for skew angle $\alpha = 45°$ and Re=100 for aspect ratio=1.5 and.

4. Summary

We have used an implicit high-order scheme for solving incompressible Navier-Stokes equations in curvilinear coordinates numerically to investigate flow in cavities. First the flow inside deep cavity is computed and comparison is given with reference solution. The effect of aspect ratio for formation of secondary vortex and critical value of aspect ratio is calculated. Second, the flow in a shallow cavity is computed and critical value of aspect ratio for two sided shallow cavity is determined. Third, it is verified that the formation of secondary vortex depends upon the aspect ratio and Reynolds number which is shown for the two-sided deep cavity flow. Fourth, the critical value of Reynolds number for non-facing cavity is determined and existence of multiple solutions above the critical value of Re is verified. Fifth, the flow behavior for skew cavities with different aspect ratios and angles are provided.
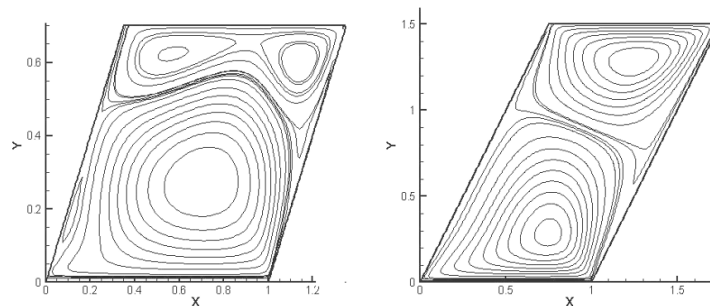

Fig. 9: The streamline pattern for two sided deep skewed cavity for parallel wall motion (left) $\alpha = 60°$, Re=1000, aspect ratio=0.75 (right) $\alpha = 45°$, aspect ratio=1.5

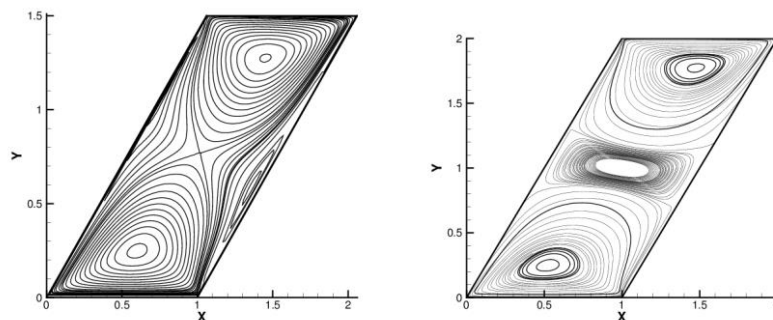**Fig. 10:** The streamline pattern for two sided deep skewed cavity for antiparallel wall motion for Re=100, $\alpha = 45°$. (left) Aspect ratio=1.5 (right) aspect ratio=2.0

References

Arun S and Satheesh A (2015). Analysis of flow behaviour in a two sided lid driven cavity using lattice boltzmann technique. Alexandria Engineering Journal, 54(4): 795-806.

Chorin AJ (1997). A numerical method for solving incompressible viscous flow problems. Journal of Computational Physics, 135(2): 118-125.

Cortes AB and Miller JD (1994). Numerical experiments with the lid driven cavity flow problem. Computers and Fluids, 23(8): 1005-1027.

Kuhlmann HC, Wanschura M, and Rath HJ (1997). Flow in two-sided lid-driven cavities: non-uniqueness, instabilities, and cellular structures. Journal of Fluid Mechanics, 336: 267-299.

Luo WJ and Yang RJ (2007). Multiple fluid flow and heat transfer solutions in a two-sided lid-driven cavity. International Journal of Heat and Mass Transfer, 50(11): 2394-2405.

Nayak RK, Bhattacharyya S, and Pop I (2015). Numerical study on mixed convection and entropy generation of Cu–water nanofluid in a differentially heated skewed enclosure. International Journal of Heat and Mass Transfer, 85: 620-634.

Omari R (2013). CFD simulations of lid driven cavity flow at moderate Reynolds number. European Scientific Journal, 9(15): 22-35.

Patil DV, Lakshmisha KN, and Rogg B (2006). Lattice Boltzmann simulation of lid-driven flow in deep cavities. Computers and Fluids, 35(10): 1116-1125.

Perumal A and Dass AK (2010). Simulation of Incompressible Flows in Two-Sided Lid-Driven Square Cavities (Part I-FDM). CFD Letters, 2(1): 13-24.

Perumal AD, Agarwal L, Raj KT, Harshan A, and Gopal NK (2014). Examination of the Lattice boltzmann method in simulation of manufactureing. ARPN Journal of Engineering and Applied Sciences, 9(4): 471-478.

Perumal DA (2012). Simulation of flow in Two-Sided Lid-Driven deep cavities by finite difference method. Journal of Applied Science in the Thermodynamics and Fluid Mechanics, 6(1): 1-6.

Perumal DA and Dass AK (2013). Application of lattice Boltzmann method for incompressible viscous flows. Applied Mathematical Modelling, 37(6): 4075-4092.

Prasad C and Dass Ak (2016). Use of an HOC scheme to determine the existence of multiple steady states in the antiparallel lid-driven flow in a two-sided square cavity. Computers and Fluids, 140: 297-307.

Shah A, Guo H, and Yuan L (2009). A third-order upwind compact scheme on curvilinear meshes for the incompressible Navier-Stokes equations. Communications in Computational Physics, 5(2-4): 712-729.

Shah A, Yuan L, and Islam S (2012). Numerical solution of unsteady Navier–Stokes equations on curvilinear meshes. Computers and Mathematics with Applications, 63(11): 1548-1556.

Wahba EM (2009). Multiplicity of states for two-sided and four-sided lid driven cavity flows. Computers and Fluids, 38(2): 247-253.